

Differential carbon utilization and asexual reproduction under elevated $p\text{CO}_2$ conditions in the model anemone, *Exaiptasia pallida*, hosting different symbionts

Kenneth D. Hoadley, Dana Rollison, D. Tye Pettay, Mark E. Warner*

School of Marine Science and Policy, University of Delaware, Lewes, Delaware

Abstract

Here we report the effects of elevated $p\text{CO}_2$ on the model symbiotic anemone *Exaiptasia pallida* and how its association with three different strains of the endosymbiotic dinoflagellate *Symbiodinium minutum* (ITS2-type B1) affects its response. Exposure to elevated $p\text{CO}_2$ (70.9 Pa) for 28 d led to an increased effective quantum yield of PSII in actinic light within two of the alga-anemone combinations. Autotrophic carbon fixation, along with the rate of carbon translocated to the animal, were significantly elevated with high $p\text{CO}_2$. Elevated $p\text{CO}_2$ exposure also coincided with significantly greater asexual budding rates in all tested anemones. Further, differences in photochemistry and carbon translocation rates suggest subtle differences in the response to $p\text{CO}_2$ among the three strains of *S. minutum* and their host anemones. This illustrates the potential for physiological diversity at the subspecies level for this ecologically important dinoflagellate. Positive alterations in photosynthesis, carbon utilization, and fitness within this model symbiosis suggest a potential benefit from ocean acidification (OA) not yet observed within corals, which may enable these anthozoans to gain a greater ecological presence under future OA conditions.

Reductions in oceanic pH, along with changes in seawater carbonate chemistry are two major physical factors resulting from rising atmospheric CO_2 concentrations that pose a threat to marine ecosystems worldwide (Guinotte and Fabry 2008). Present day atmospheric partial CO_2 pressure ($p\text{CO}_2$) is already much higher than the previous 800,000 yr (Luthi et al. 2008), and under current CO_2 emission rates, is predicted to double by the end of this century (IPCC 2013). These changes in pH and carbonate chemistry as a result of increasing $p\text{CO}_2$, commonly referred to as ocean acidification (abbreviated as OA hereafter), are especially important for marine organisms reliant on dissolved inorganic carbon (DIC) for photosynthesis and/or calcification (Iglesias-Rodriguez et al. 2008; Hurd et al. 2009; Hofmann et al. 2010). Understanding how such organisms respond to OA is critical toward predicting the future state of marine ecosystems.

For many marine photosynthetic organisms the increase in DIC resulting from rising CO_2 emissions may be beneficial, promoting greater rates of primary productivity due to enhanced carbon availability (Koch et al. 2013). For example, some seagrass species are positively affected by OA, with productivity rates and carbon sequestration increasing significantly (Zimmerman et al. 1997; Alexandre et al. 2012),

while increased productivity and growth have also been documented for several phytoplankton species as well (Xia and Gao 2005; Hutchins et al. 2007; Beardall et al. 2009). Conversely, reductions in pH and carbonate ions may pose a significant problem for marine organisms that produce calcium carbonate skeletons or shells. With respect to OA, scleractinian corals are a unique group, as they contain both intracellular symbiotic dinoflagellates and produce a calcium carbonate skeleton, and hence possibly experience both negative and positive effects of OA. The importance of their carbonate skeleton, in particular to reef accretion, has led many researchers to focus on how calcifying corals respond to OA. Although research is ongoing, recent studies suggest that the response is species specific and for some species, no change or only small reductions in rates could be expected with elevated $p\text{CO}_2$ (Comeau et al. 2013; Edmunds et al. 2013; Schoepf et al. 2013). With respect to photophysiology, reductions in cell density and net photosynthesis due to elevated $p\text{CO}_2$ have been reported for some calcifying coral species (Kaniewska et al. 2012) but not others (Crawley et al. 2010; Wall et al. 2014). Importantly, increases in gross photosynthesis have also been reported (Suggett et al. 2012a) thereby illustrating the broad mix of photophysiological responses to $p\text{CO}_2$ among different scleractinian coral species.

*Correspondence: mwarner@udel.edu

While the impacts of OA have been investigated in many species of reef-building coral, less attention has been given to non-calcifying soft-bodied anthozoans such as sea anemones. In a natural experiment along a CO₂ seep off the coast of Italy, the anemone *Anemonia viridis* significantly increased its growth, size and primary productivity rates near high CO₂ seep locations (Suggett et al. 2012b), while laboratory experiments with *Anthopleura elegantissima* and *Exaiptasia* sp. (temperate and tropical, respectively) have noted increased oxygen production with elevated pCO₂ in both anemones (Towanda and Thuesen 2012; Gibbin and Davy 2014). Together these studies suggest that anemones may, in fact, benefit significantly from OA. Disturbance induced community phase-shifts from scleractinian corals toward other symbiotic cnidarians, such as anemones, have been noted (Norstrom et al. 2009; Dudgeon et al. 2010). In contrast, the prevalence of soft-bodied corals declined with proximity to natural CO₂ seeps off the coast of Papua New Guinea (Fabricius et al. 2011). Whether or not soft-bodied symbiotic anthozoans are better able to acclimatize to climate change will become an increasingly important question as sea surface temperatures and pCO₂ continue to rise.

The sea anemone *Exaiptasia pallida* (formerly *Aiptasia pallida*, see Grajales and Rodríguez (2014)) is rapidly becoming an important model organism for the study of cnidarian-*Symbiodinium* symbioses (Sunagawa et al. 2009; Lehnert et al. 2012; Voolstra 2013). Associations with the same genera of dinoflagellates as reef corals, ease of culturing, and rapid rate of asexual reproduction make *E. pallida* an ideal system for studying symbiotic anthozoans. In nature, *E. pallida* is globally distributed and maintains natural symbioses with only a select subset of *Symbiodinium* species (Thornhill et al. 2013). However, these anemones are easily maintained in the laboratory without symbionts (i.e., aposymbiotic) and subsequently “infected” with a genetically diverse set of *Symbiodinium* species (Schoenberg and Trench 1980). The ability to host divergent and specifically chosen symbionts provides a unique opportunity to understand the influence of symbiont identity on the host’s response to environmental stress such as OA.

The genus *Symbiodinium* is a highly diverse group of photosynthetic dinoflagellates that form complex associations with a range of host taxa from multiple phyla (Trench 1993; Coffroth and Santos 2005; Sampayo et al. 2009). Although our understanding of the genetic diversity and biogeography of this genus has outpaced that of the comparative physiology, their response to environmental stress can vary greatly among symbiont lineages or groups (Iglesias-Prieto and Trench 1997; Warner and Berry-Lowe 2006; Hennige et al. 2011). Therefore, the dominant symbiont can dramatically affect the host’s response to environmental stress (e.g., Sampayo et al. 2008; Grottoli et al. 2014). Genetic characterization of *Symbiodinium* by nuclear, chloroplast and mitochondrial markers currently divides this genus into nine

clades (designated by the letters A–I) with each clade containing additional diversity that is resolved using more variable markers such as the ribosomal internal transcribed spacer (ITS) regions (Santos et al. 2003; Coffroth and Santos 2005; Sampayo et al. 2009). While, in some cases, diversity in the ITS regions equates approximately to a species-level designation, the recent use of microsatellite loci provide even finer resolution at the sub-species level, enabling the ability to distinguish different clonal variants or individuals (i.e., multilocus genotypes) within a species (Pettay and LaJeunesse 2007; Pettay and LaJeunesse 2009; Wham et al. 2011). These loci have revealed substantial diversity within individual symbiont species and population patterns that mirror changes in the prevailing environmental conditions (e.g., sea surface temperature), suggesting important physiological differences exist even at the sub-species level (Pettay and LaJeunesse 2013). However, few studies to date have attempted to characterize physiological differences among genetically distinct clonal variants of a *Symbiodinium* species (Leal et al. 2015), or how they interact with the host organism’s response to physical stress while in hospite.

The aim of this study was to investigate the response of different anthozoan holobionts (used here to define the host + algal symbiont) to OA by utilizing the *Exaiptasia* model system. Throughout its global distribution *E. pallida* associates predominantly with the clade B symbiont, *Symbiodinium minutum* (LaJeunesse et al. 2012; Thornhill et al. 2013). Therefore, three genetically distinct clonal variants of *S. minutum* were chosen to quantify within-species physiological variability and the overall holobiont response to elevated pCO₂. Subtle differences in photochemistry and physiology were detected and influenced how each host/symbiont combination responded to ocean acidification. This work represents the first characterization of sub-species physiological differences in *Symbiodinium* and their influence on holobiont response to changes in pCO₂.

Materials and methods

Development of host/symbiont combinations

All anemone/symbiont combinations were maintained in stable symbiosis for approximately one year prior to use in this experiment. Aposymbiotic *E. pallida* (clone CC7, donated by J. Pringle, Stanford University) (Sunagawa et al. 2009) were held in glass bowls and “infected” with one of two cultured strains of *S. minutum* (referred to as strains 1 and 2, respectively; Table 2). In addition, a subset of aposymbiotic anemones was maintained under 12 : 12 hour light : dark (100 μmol quanta m⁻² s⁻¹) conditions to ensure that no remaining symbionts were present and could repopulate the host. After 3 months, microscopic visualization showed no signs of repopulation for any of the aposymbiotic anemones tested. Algal isolates utilized for infection were originally isolated from *E. pallida* from Florida and from a

Caribbean gorgonian (*Plexaura kuna*) (isolates FLAp2 and Pk704, respectively from the BURR culture collection, donated by M. A. Coffroth, University of Buffalo). *S. minutum* belongs to the clade B lineage and is also known as type B1 by characterization of the ITS2 sequence (LaJeunesse 2001). The B1 lineage contains multiple genetic groupings that approximate species-level diversity and roughly correspond to host associations (Finney et al. 2010; LaJeunesse et al. 2012). For initial infections, anemones were exposed to approximately 1 mL algal culture (10,000–100,000 cells mL⁻¹ in log-phase growth) for 48 h, followed by a 100% water change with filtered seawater. Anemones were inspected daily under a dissecting microscope, and all anemones appeared to harbor symbionts within their tentacles in the first 24 h of algal exposure. Once symbiotic, each *Exaiptasia*/alga combination was held in separate 19 L flow through aquaria that received filtered (1 µm) and UV-treated seawater and 100 µmol quanta m⁻² s⁻¹ photosynthetically active radiation (PAR) provided by cool-white fluorescent lights on a 12 : 12 light : dark cycle. All anemones were fed *Artemia* nauplii twice each week. In addition to the CC7 *Exaiptasia* clone, a third, naturally occurring *Exaiptasia*/*S. minutum* symbiosis (referred to as “strain 3”) was originally collected from Bermuda and also maintained under the same conditions.

Genetic analysis of symbionts and host

Prior to the experiment and anemone infection, each cultured symbiont was genetically characterized using PCR-DGGE of the partial 5.8S and internal transcribed spacer 2 (ITS2) region of the ribosomal array (LaJeunesse 2002). In addition, the flanker region sequence of the microsatellite locus B7Sym15 was sequenced to verify the placement of these algae within the species *S. minutum* (LaJeunesse et al. 2012), and further genetic analyses using microsatellite loci for clade B *Symbiodinium* were conducted to delineate and verify strain identity in each symbiosis. Five haploid loci were analyzed (Table 2) according to Pettay and LaJeunesse (2007) to create a multilocus genotype (MLG) for each strain. Following the experiment, five replicate anemones for each symbiont combination from both the treatment and control ($n = 10$ total combination) were analyzed to confirm the stability of the symbioses at both the ITS2 and MLG level of resolution.

In addition to the symbionts, both host anemone populations (CC7 and Bermuda strain) were genetically characterized using newly developed microsatellites for *E. pallida* to verify each line was genetically distinct (Table 3) (Pettay and Grajales unpubl.). Briefly, microsatellite loci were developed from EST sequences of *E. pallida* (Sunagawa et al. 2009) that were vectored screened (using VecScreen and the UniVec NCBI vector library) and assembled (CAP3; Huang and Madan 1999). Contigs and singlet sequences were screened for simple sequence repeats (SSRs) of di, tri, tetra, penta and

hexanucleotides with more than six repeats (WebSat; Martins et al. 2009). Primers were designed for candidate loci (Primer3; Rozen and Skaletsky 1999) and the loci screened on *E. pallida* samples from the Florida Keys and Bermuda collected in 2011. The loci were amplified following (Pettay and LaJeunesse 2007) and their descriptions are given in Table 3.

Experimental design

Small glass bowls (9 cm diameter, 130-mL volume) covered with 300 µm nitex mesh tops were used to hold different anemone/symbiont combinations. Each glass bowl held four anemones, with five glass bowls per host/symbiont combination in each treatment. One glass bowl per host/symbiont combination was placed in each of five replicate aquaria per treatment (described below). To lessen possible tank effects, the position of each bowl within each tank was changed every day, and bowls were moved to a different aquarium every 3rd day. After an initial 5 d of acclimation to the experimental systems, each treatment ran for 28 d. Anemones were not fed during the 28-d experiment. All bowls and mesh tops were gently cleaned of any fouling debris two times each week.

Each recirculating treatment system consisted of five, 15 L aquaria connected to a central 416 L sump with flow rates in each aquarium of ~ 567 L h⁻¹. Anemones were maintained under a 12 : 12 h light : dark cycle, using a customized uniform LED array (Cree XPG-R5, cool white; 5000–8300 K) that simulated a diel light cycle by ramping light intensity from 10 µmol photons m⁻² s⁻¹ to 200 µmol photons m⁻² s⁻¹ each day using an Apex Junior AquaController (Neptune Systems). Lights were ramped up from 10 µmol photons m⁻² s⁻¹ to 200 µmol photons m⁻² s⁻¹ over a 3 h period, maintained at 200 µmol photons m⁻² s⁻¹ for 6 h and then ramped back down from 200 µmol photons m⁻² s⁻¹ to 10 µmol photons m⁻² s⁻¹ over 3 h before turning off for 12 h. Temperature was maintained at 26.5°C using titanium heaters housed in each sump and also regulated using an Apex AquaController. Salinity was maintained at 32 psu using a float valve and RO water. Temperature (26.5°C) and salinity were manually confirmed every other day. To minimize variability in seawater chemistry, a 40% water change was performed on each system every other day using filtered and UV sterilized natural seawater collected at the Delaware Indian River inlet during the incoming tide.

CO₂ treatments consisted of ambient (35 Pa) and elevated (70.9 Pa) pCO₂ to represent the current (for the DE water) and predicted conditions expected by the mid to late 21st century (IPCC 2013) and were maintained using a pH stat system for precise control of air and CO₂ gas input (KSGrowstat, University of Essex). To ensure stability of carbonate chemistry throughout the experiment, pH measurements were taken within each treatment sump every 120 s with a glass microelectrode (Thermo Scientific, Orion Ross Ultra pH glass electrode) that was connected to a pH electrode

Table 1. Average conditions for each treatment. Mean \pm 1 SE are shown. All seawater carbonate chemistry based on pH and Alkalinity measurements was calculated using the CO2SYS program (Lewis et al. 1998).

	Ambient CO ₂	High CO ₂
Temp. (°C)	26.81 \pm 0.1108	26.78 \pm 0.1437
pH _T	8.22 \pm 0.018	7.95 \pm 0.013
pCO ₂ (Pa)	35 \pm 0.1	70.9 \pm 0.15
TA (μ mol kg ⁻¹)	2164 \pm 44	2073 \pm 3
X _{arag}	3.37 \pm 0.01	1.97 \pm 0.005
Salinity (ppt)	33.36 \pm 1.2	33.09 \pm 1.3

amplifier (PH 02, Technologica Ltd., U.K.). The pH signals were then processed by computer, which then controlled a series of solenoids designed to deliver CO₂, air or CO₂-free air. The microelectrodes were recalibrated each day using NBS calibration buffers and confirmed through independent measurements of pH using a Fischer Scientific A815 Plus pH meter. In addition, pH and total alkalinity (TA) was monitored over several daily cycles and representative data are shown (Table 1). TA was measured using a bromocresol purple based colorimetric assay according to (Yao and Byrne 1998) with a spectrometer set in absorbance mode (Ocean Optics, USB4000-ES) and a titrator (Metrohm 876 Dosimat plus, Switzerland). Parameters for seawater carbonate chemistry based on pH and alkalinity measurements were calculated using the CO2SYS program (Lewis et al. 1998) and are reported in Table 1.

Host and symbiont physiology

Chlorophyll a fluorescence

Dark acclimated maximum quantum yield of photosystem II ($F_v : F_m$) was measured every 3 d, 1 h after the light period by pulse amplitude modulation fluorometry (Diving PAM, Waltz, Germany). In addition, the effective quantum yield, ($F_q : F_m$, also known as the operating efficiency of PSII) was also measured on the final day, during midday under the LED lights.

Anemone preservation and processing

Asexual reproduction, (budding) rates, were calculated by counting the total number of new recruits within each bowl each week and were then combined to represent the collective reproductive effort of the four original anemones placed within each bowl (number of buds per month). After physiology measurements at the end of the experiment, all anemones were flash frozen in liquid nitrogen and then stored at -80°C until further processing. For processing, anemones were ground in 1 mL of seawater using a 1.5 mL tenbroeck glass tissue grinder, and then centrifuged (5000 \times g) for 5 min. Soluble animal protein (mg mL⁻¹) was determined from two replicate 50 μ L samples of the animal supernatant, using a BCA Protein kit (Thermo Scientific Pierce), with

bovine serum albumin used for standards (Smith et al. 1985). The algal cell pellet was re-suspended in 400 μ L of seawater and separated into two 200 μ L aliquots, for algal cell density and chlorophyll *a* (Chl *a*) quantification. Samples for algal cell counting were preserved with 10 μ L 1% glyceraldehyde and manually counted by light microscopy, using a hemocytometer (six independent replicate counts) under 100X magnification. Total protein concentrations for each anemone/symbiont combination were not significantly different between treatments or among host/symbiont combinations (not shown). Therefore any differences observed in algal cell density are not likely influenced by CO₂ induced changes in animal protein concentration. Chl *a* was extracted by bead beating cells (BioSpec) using 0.5 mm glass beads for 60 s in chilled 90% methanol. Samples were then incubated at -20°C overnight, followed by centrifugation to remove remaining debris. Chl *a* concentration was then determined spectrophotometrically (Porra et al. 1989).

Carbon uptake and translocation

Individual anemones were placed in separate 7 mL scintillation vials containing 2 mL of seawater spiked with 15 μ L of ¹⁴C-labeled bicarbonate (specific activity 17 μ Ci μ mol⁻¹). Five anemones were used for each host/symbiont combination and treatment. Vials were placed on a LED₂ light-table (Cool White Cree XPG-R5; 600 μ mol photons m⁻² s⁻¹; 28°C) for 90 min. Short-term exposure to this light level resulted in no significant change in maximal photosynthesis in control anemones grown at 200 μ mol photons m⁻² s⁻¹ (data not shown). An additional two anemones from each treatment and host/symbiont combination were placed in vials with ¹⁴C-spiked seawater and held in the dark for 90 min to account for carbon uptake in the dark. Three additional vials containing only the spiked seawater were also included for measurement of total activity.

After ¹⁴C incubations, the total organic carbon (TOC) released, which is comprised of both particulate and dissolved organic carbon (POC and DOC) released by each holobiont, was calculated by first mixing each vial to ensure a homogenous sample, and then removing 200 μ L of seawater for TOC calculations. Each anemone was then removed from the vial and ground in 1 mL of seawater in a 1.5 mL glass tenbroeck tissue grinder. A 100 μ L sample of the resulting homogenate was removed and fixed with 10 μ L 1% glutaraldehyde and used for algal cell counts as described above. The remaining homogenate was centrifuged (5000 \times g) for 5 min to separate the host and symbiont portions. The supernatant was completely removed, and a 500 μ L subsample was utilized for measuring carbon translocated to the host (H_s), while the remaining supernatant was used for calculating host protein content. The remaining algal cell pellet was resuspended in 500 μ L of FSW, vortexed, and then centrifuged again to extract any remaining host supernatant (RH_s) from the algal pellet. The algal pellet (S) was then

Table 2. Description of the Symbiodinium minutum cultures, including their host of origin, host used and their five-locus genotypes. Strain identify for each anemone host used here is provided in parentheses.

Strain	Culture name	Original host	Host used	Microsatellite fragment sizes (bp)*				
				B7Sym15	B7Sym34	B7Sym36	CA4.86	CA6.38
1	FLAp2	Exaiptasia pallida	Exaiptasia pallida (CC7)	263	281	196	182	101
2	PK704	Plexaura kuna	Exaiptasia pallida (CC7)	263	267	163	199	103
3	N/A	Exaiptasia pallida	Exaiptasia pallida (Bermuda)	259	271	169	182	101

*Loci B7Sym15, B7Sym34 and B7Sym36 from Pettay and LaJeunesse (2007), while loci CA4.86 and CA6.38 from Santos and Coffroth (2003).

resuspended a final time in 400 μ L of FSW. All samples measured for radioactivity were acidified with an equal volume of 0.1 mol L⁻¹ HCl, placed in 7 mL scintillation vials for 24 h and then combined with 5 mL of scintillation cocktail (Ultima Gold, Perkin Elmer) prior to reading with a liquid scintillation counter (Beckman LS-6500). Samples were corrected for background activity and dark incorporation. All sample measurements and calculations follow previously established methods for *E. pallida* (Davy and Cook 2001). Translocation and photosynthesis rates were determined by the average specific activity (g C dpm⁻¹) and the duration of the incubation. The fraction of carbon translocated (T_L) was calculated as,

$$T_L = \frac{TOC + H_s + RH_s}{TOC + H_s + RH_s + S}$$

and then normalized algal cell number and to host protein, where TOC is the total organic carbon and H_s and RH_s are the host supernatant and remaining host supernatant, respectively.

The fraction of carbon produced from net photosynthesis (P_{net}) was normalized to algal cells anemone and calculated as,

$$P_{net} = \frac{TOC + H_s + RH_s + S}{TOC + H_s + RH_s + S}$$

where S is the algal pellet described above.

Using the ratio of the portions described above, the fraction of photosynthate translocated to the host was calculated as,

$$T_L P_{net} = \frac{(TOC + H_s + RH_s)}{(TOC + H_s + RH_s + S)}$$

Statistical analysis

All datasets were tested for assumptions of homogeneity of variance and normality of distribution using the Levene and Shapiro–Wilk tests, respectively. If either test invalidated these assumptions, the data was log transformed and retested to ensure normality prior to further analysis. A two-way analysis of variance (ANOVA) was used to test for significant effects of the main variables pCO_2 and symbiont type and the interactive effects between the two ($\alpha = 0.05$). If significant differences in host: symbiont combination was observed, a Tukey post hoc test was utilized to distinguish

significant difference among the three types. If interactive effects were observed, all other main effects were ignored and the analysis was followed up with a pairwise analysis of all six groups. Budding rate data were non-normal after transformation and samples were tested by a Kruskal–Wallis test with multiple comparisons. For maximum quantum yield of PSII ($F_v : F_m$), separate two-way repeated measures ANOVAs were utilized to test for significant differences among treatments within each symbiont type. A Mauchly’s test was also performed to check and correct for violations of sphericity. If significant differences were observed, the analysis was followed up with a paired t -test on each day. All statistical analyses were performed using the open source software R with “car” and “pgirmess” packages installed (<http://www.R-project.org/>).

Results

Host/symbiont identity and stability

All three strains of symbionts were verified as ITS2-type B1 and *S. minutum*, as defined by the ITS2 sequence that dominates their ribosomal array (Genbank# AF333511) and flanker region sequence of B7Sym15 (Genbank# JX263427), respectively. The clonal lines of *E. pallida* maintained stable associations with each *S. minutum* strain for the duration of culturing and exposure to experimental conditions. The three different strains of *S. minutum* were genetically distinct and differed by as many as five alleles for pairwise comparisons of their microsatellite derived haploid MLGs and were designated as strains 1, 2, or 3 (Table 2). The two *E. pallida* clonal lines were distinct and differed by at least one allele at all six loci except AIPT14 (Table 3). These genetic lineages led to holobiont combinations of the *E. pallida* clone CC7 with *S. minutum* strains 1 and 2, and the Bermuda *E. pallida* clone with *S. minutum* strain 3.

Photosynthesis, carbon uptake and symbiont physiology

Elevated CO_2 significantly affected anemone/algal symbioses, with changes occurring at the photochemical, cellular and organismal level. Significant time effects were observed for anemones with strain 1 ($p = 0.003$) and 3 ($p = 0.003$) as maximum quantum yields ($F_v : F_m$) varied throughout the experiment but no significant treatment effect was observed by the end of the experiment in two of the holobionts

Table 3. Description of the six *Exaiptasia pallida* microsatellite loci and MLGs of the two *E. pallida* clones.

Locus	Primer	Repeat	A _T	Accession #	CC7 Clone	Bermuda Clone
AIP6	F-(HEX)GAATCAGGAATCAACCCAACAT	(TGA) ₇	59°C	GH577343	302	302
	R-TAAGTGCCAGACCAACAACAAC				302	318
AIP8	F-(FAM)AAAAGATTTCGTGAGCAGAAAGG	(TA) ₆	59°C	GH574595	293	293
	R-GAGCTGAAATAAGGTGAATACAAGG				295	293
AIP14	F-(FAM)AAAAGATTGAAGACGAACCAGC	(GCA) ₇	59°C	GH578373	188	188
	R-ATAACTGGGCATTCCACCATAC				191	191
AIP15	F-(HEX)TCAGCAGTACGGAGGAATGAAC	(CCA) ₇	59°C	GH578373	319	319
	R-AGGAGGGCACGGTTGTTG				322	319
AIP17	F-(HEX)GCTACTTTACCCGAACCCAAG	(TA) ₆	59°C	GH573936	292	294
	R-TAGACGACTTGCGAGATCAAAA				292	296
AIP20	F-(FAM)GACTGGCACATTACCATCTATAACA	(AT) ₇	59°C	GH578509	334	339
	R-AGTTAGTTGTGTGGTTGCCCT				334	341

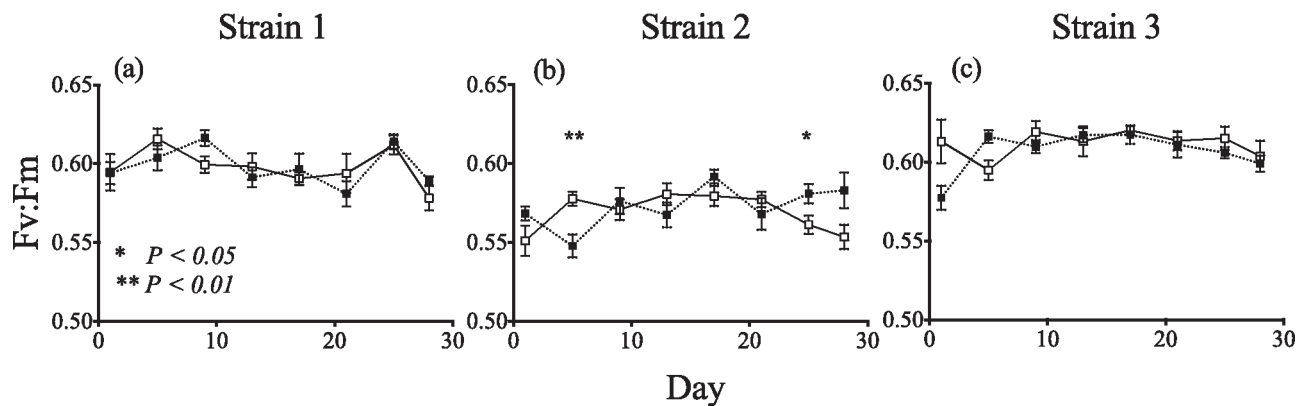


Fig. 1. Maximum quantum yield of PSII in three different *Exaiptasia*-*Symbiodinium* combinations under ambient and elevated CO₂ (a–c). Mean \pm 1 SE are shown for ambient and elevated pCO₂ (35 Pa = light symbols, 70.9 Pa = dark symbols). Asterisks represent significant differences (* $p < 0.05$; ** $p < 0.01$) between the ambient and high CO₂ treatments on that day.

(Fig. 1a,c). However there was a significant interactive effect for strain 2 ($p = 0.013$), as maximum quantum yields also varied throughout the experiment, with significant CO₂-induced decreases on day 5 ($p = 0.008$) followed by a significant increase by day 25 ($p = 0.04$) (Fig. 1b). Exposure to elevated CO₂ resulted in a small yet significant increase in the effective quantum yield of PSII in the light ($F_v : F_m$) ($p = 0.001$) in anemones hosting strains 1 and 2 (Fig. 2a). Additionally, differences among the host: symbiont combinations were also observed as anemones hosting strain 3 were significantly elevated over strain 1 ($p = 0.0001$) and strain 2 ($p < 0.0001$). Although the difference was minimal, strain 1 $F_v : F_m$ was significantly higher than strain 2 ($p = 0.001$). In addition to these changes in PSII photochemistry, net photosynthesis algal cell significantly increased with elevated pCO₂ in all anemones ($p < 0.001$) (Fig. 2b).

While there was no significant main effect of elevated CO₂ exposure on symbiont density, a significant interactive effect ($p = 0.016$) was noted, as patterns in algal cell density

differed among the anemone/algal combinations, with symbiont density declining in strains 2 and 3 and rising marginally for strain 1 under the high CO₂ treatment. Symbiont density for the strain 3 holobiont were also significantly higher than strain 1 under ambient but not elevated pCO₂ (Fig. 2c). At ambient CO₂, Chl *a* content also varied significantly with symbiont type ($p < 0.001$), with strain 1 having a greater concentration of Chl *a* algal cell than strain 2 ($p < 0.001$) and strain 3 ($p = 0.002$). However, there was no significant change in cellular Chl *a* under elevated CO₂ (Fig. 2d).

Translocation and host reproduction

The percent of carbon translocated to the host differed significantly among holobionts under the ambient CO₂ treatment ($p = 0.002$), with anemones hosting strain 3 receiving a significantly lower portion of photosynthate than animals hosting strain 1 or strain 2 algae ($p = 0.028$, $p = 0.001$, respectively) (Fig. 3a). Meanwhile, the simple means effect of

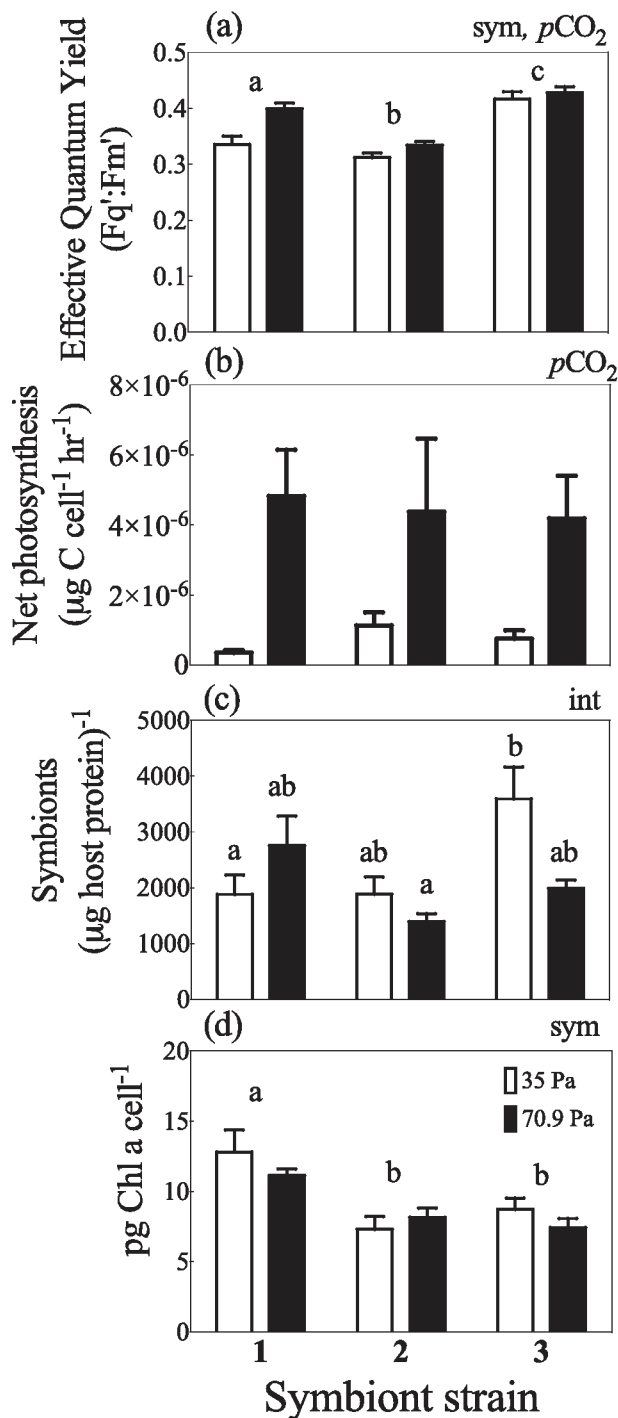


Fig. 2. Effective quantum yield (a), Net photosynthesis (b), symbiont cell density (c), and Chl a cell⁻¹ (d). Mean ± 1 SE are shown for ambient and elevated pCO₂ (35 Pa = light bars, 70.9 Pa = dark bars). The abbreviations (sym), (pCO₂) and (Int) in the top right corner of each plot indicate significant differences between symbiont strain, pCO₂ or interactive effects resulting from a two-way ANOVA (n = 5). If a pCO₂ effect was observed, the letters indicate significant differences between pCO₂ groups (n = 5 ± SE). If an interactive effect was observed, the letters above each bar indicate significant differences among the six treatments.

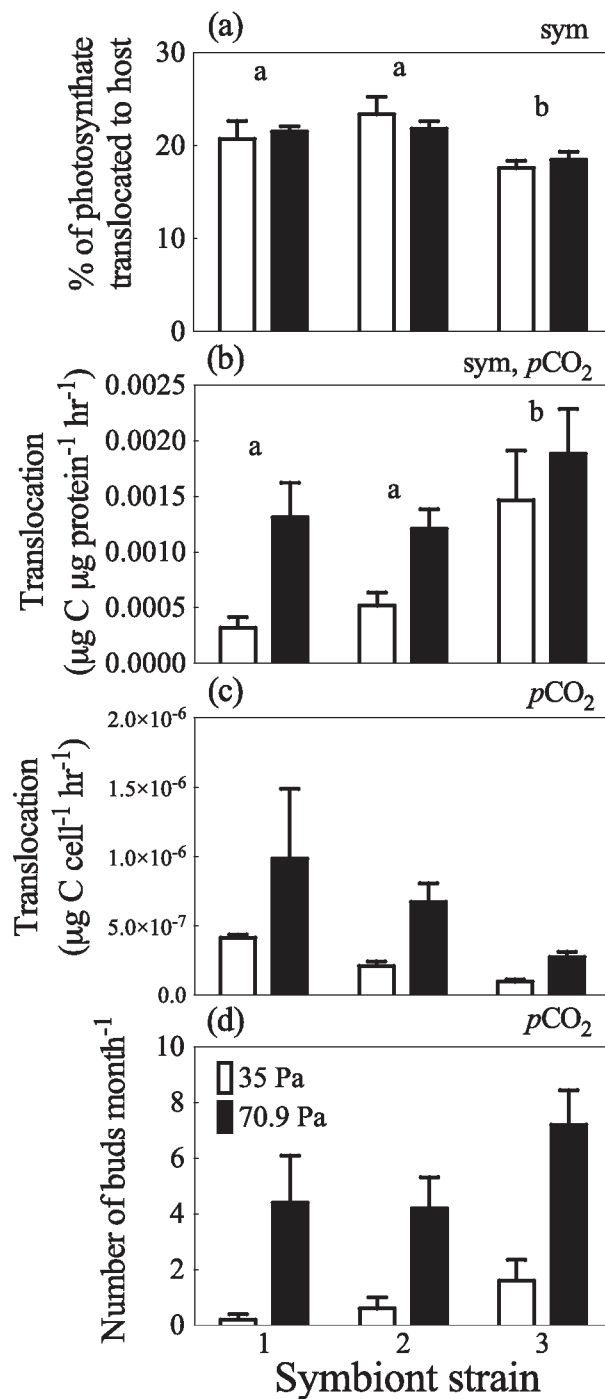


Fig. 3. Percent of photosynthate translocated to the host (a), carbon translocation rate normalized to the host protein (b), carbon translocation rate normalized to algal cell number (c), and the number of asexual anemone buds produced month⁻¹ (d). Mean ± 1 SE are shown for ambient and elevated pCO₂ (35 Pa = light bars, 70.9 Pa = dark bars). The abbreviations (sym), (pCO₂) and (Int) in the top right of each plot indicate significant differences between symbiont, pCO₂ or interactive effects resulting from a two-way ANOVA (n = 5). Significant differences among strains are denoted by the letters above each treatment group (n = 5 ± SE).

the two way ANOVA found a significant increase with $p\text{CO}_2$ ($p < 0.001$) for translocation rates to the host (expressed as $\mu\text{g carbon} \mu\text{g host protein}^{-1} \text{h}^{-1}$), driven primarily by increases within strains 1 and 2 (Fig. 3b). The host: symbiont combination was also a factor, as strain 3 translocation rates were significantly elevated over strains 1 ($p = 0.003$) and 2 ($p = 0.027$) and most notably at ambient $p\text{CO}_2$. A significant ($p = 0.030$) CO_2 induced increase in carbon translocation was also observed when rates were normalized to symbiont cell density ($\mu\text{g carbon released cell}^{-1} \text{h}^{-1}$) (Fig. 3c). Lastly, elevated $p\text{CO}_2$ exposure led to a significant increase in the rate of asexual reproduction ($p < 0.05$) in all strains.

Discussion

Elevated $p\text{CO}_2$ designed to mimic mid to late 21st century conditions over 28 d (70.9 Pa $p\text{CO}_2$) resulted in substantially increased photosynthetic carbon uptake for all three strains of *S. minutum*. Similar increases in photosynthesis (as measured by respirometry) were observed for the temperate symbiotic anemone *Anthopleura elegantissima* during a 6-week exposure to $p\text{CO}_2$ of 230.9 Pa (Towanda and Thuesen 2012) and *Exaiptasia* sp. exposed to $p\text{CO}_2$ of 69.6 Pa and 147.8 Pa (Gibbin and Davy 2014). In the natural environment, growth and abundance of the symbiotic sea anemone *Aneemonia viridis* increased along a natural volcanic CO_2 seep in Italy, suggesting a significant benefit from elevated $p\text{CO}_2$ for this species as well (Suggett et al. 2012b). Together, these studies suggest a beneficial effect of elevated $p\text{CO}_2$ on sea anemones, and further that their photosynthetic symbionts may be carbon limited under ambient $p\text{CO}_2$ conditions.

Elevated dissolved inorganic carbon (DIC) associated with OA is hypothesized to enhance photosynthetic rates for carbon limited endosymbionts (Langdon and Atkinson 2005; Cohen and Holcomb 2009). Similar to early work with free-living phytoplankton where it was assumed that carbon limitation did not play a role, subsequent studies have observed increases in productivity associated with elevated DIC within a number of free-living phytoplankton, suggesting that carbon limitation may play an important role in productivity rates within the open-ocean as well (Xia and Gao 2005; Fu et al. 2007; Hutchins et al. 2007; Beardall et al. 2009). Earlier work with *E. pallida* by Davy and Cook (2001) observed an increase in net photosynthesis and photosynthate translocation (normalized to algal cell number) after 20–30 d of starvation. During this time, there was a notable decline in symbiont densities in these starved anemones, and the noted increase in net photosynthesis and carbon translocation was thought to result from greater carbon availability per algal cell (Davy and Cook 2001; Wooldridge 2009). These changes in carbon incorporation point toward DIC limitation within *Symbiodinium* as previously described by (Weis 1993), where net photosynthesis also increased with elevated DIC concentrations within *Aiptasia pulchella*. The substantial rise in net

photosynthesis for all three strains of *S. minutum* noted here also supports this hypothesis. Interestingly, *Symbiodinium B1* isolates in culture (presumably closely related to *S. minutum*) (Brading et al. 2011) showed no increase in net photosynthesis in response to elevated $p\text{CO}_2$. This discrepancy among closely related symbionts grown in culture vs. in hospite may indicate a greater reliance on host carbon concentrating mechanisms (Leggat et al. 1999) and/or that free-living *Symbiodinium minutum* strains are not DIC limited (Brading et al. 2011).

Along with a major increase in carbon uptake cell^{-1} , PSII photosynthetic efficiency remained relatively stable under high $p\text{CO}_2$ conditions within strains 1 and 3, with only a slight increase toward the end of the experiment in strain 2 (Fig. 1). In contrast the effective quantum yield (i.e., operating efficiency of PSII in the light) did increase significantly (although only slightly in strain 2 and 3) under elevated CO_2 conditions. Photosynthesis in *E. pallida* tends to saturate at light levels near $200 \mu\text{mol photons m}^{-2} \text{s}^{-1}$ (Muller-Parker 1984; Goulet et al. 2005). Therefore, it is likely that anemones used here were light saturated and well poised to take advantage of the greater electron sink provided by elevated carbon availability. As with other marine phytoplankton, the photosynthetic response to elevated $p\text{CO}_2$ may differ significantly under low light conditions where photosynthetic electron flow rather than carbon availability is the rate-limiting step in photosynthesis (Li and Campbell 2013). Reductions in calcification and photosynthesis were greater under low as opposed to high light conditions under elevated $p\text{CO}_2$ for the corals *A. horrida* and *P. cylindrica* and suggest that OA alleviated $p\text{CO}_2$ limitation under high light conditions (Suggett et al. 2012a). It is therefore possible that under lower light levels, the *S. minutum* response to elevated $p\text{CO}_2$ could differ significantly than presented here.

Despite increased photosynthetic productivity and in contrast to the work of Gibbin and Davy (2014) and Suggett et al. (2012b), there was no significant change in the *S. minutum* density in any anemone/algal pairing in response to elevated $p\text{CO}_2$. A drop within strain 3 was apparent, however this was not significant. Towanda and Thuesen (2012) also noted no change in symbiont density for the temperate anemone, *A. elegantissima*, held under two OA scenarios for approximately double the time period used here (Towanda and Thuesen 2012). This may reflect some decoupling between increased productivity and cell density, as *Symbiodinium* spp. are typically in severe unbalanced growth in hospite and release a significant portion of their photosynthetically fixed carbon to the host (Dubinsky and Berman-Frank 2001). Such changes in symbiont density under excess CO_2 could reflect a change in the balance of carbon and nitrogen supply to the alga and the host, similar to patterns noted for nitrogen limitation in these symbioses. For example, Marubini and Davies (1996) noted a significant increase in algal density after exposure to excess nitrogen.

While Gibbin and Davy (2014) did note higher algal density with increased $p\text{CO}_2$, this was at a CO_2 concentration double that utilized here (~ 147 Pa). Additionally, natural CO_2 levels yielding the largest response in Suggett et al. (2012b) were also considerably higher (144.7 Pa).

An increase in net photosynthesis led to a similar rise in translocation rates (per algal cell) at elevated $p\text{CO}_2$ for all three symbiont strains. From the host perspective, however, greater carbon translocation rates (per host protein) only occurred for anemones hosting algal strains 1 and 2 (Fig. 3b), with a loss in cell density by strain 3 counteracting any potential gain in photosynthate contributed to the host. Higher percent of translocated carbon, but lower photosynthetic rates, were observed under extremely high CO_2 concentrations (394.9 Pa) in the scleractinian coral *Stylophora pistillata* (Tremblay et al. 2013). Unlike our findings for *E. pallida*, the increase in percent translocation to *S. pistillata*, despite a decline in photosynthesis, may indicate an important change in the symbiosis that is not conducive toward sustained growth and health or represent an important difference between calcifying and non-calcifying cnidarians. Alternatively, the differences may be attributed to the large difference in the $p\text{CO}_2$ treatments used in these two studies (70.9 vs. 394.9 Pa).

Interestingly, the carbon translocation rate of the anemone hosting the strain 3 alga was significantly higher than the other two host/symbiont combinations despite a smaller percentage of the total photosynthate produced being shared with the host anemone (Fig. 3a,b). As data presented here were normalized to host protein, it is possible that changes in total protein concentration could influence our understanding of carbon translocation to the host and bias such results. However, no significant differences in total protein per anemone were observed between treatments or among host/symbiont combinations (data not shown). Furthermore, the anemones hosting strains 1 and 2 were from the same clonal line whereas the anemone with strain 3 was a different host genotype, and the differences in photosynthate allocation likely reflect distinct differences in the overall symbioses among the three anemone : symbiont combinations tested here (Leal et al. 2015). These differences in the symbioses may play an even greater role under more severe stressors such as elevated temperature and underscore the need to assess the genetic identity of the alga and animal in such studies. In addition, the use of ^{14}C to measure carbon translocation cannot account for rapidly respired autotrophically derived carbon (Tremblay et al. 2013). It is therefore possible that changes in respiration rates could also underestimate differences in rates of carbon translocation observed here.

While the percentage of photosynthate translocated by the symbionts remained the same, host budding rates increased significantly with elevated $p\text{CO}_2$. Previous work by Clayton (1985) and Clayton and Lasker (1985) showed that

asexual budding rates by *Aiptasia* sp. lead to greater rates of biomass accumulation than host tissue growth, allowing for a clonal population to quickly increase. This is likely due to the relatively cheap reproductive effort required for pedal laceration (asexual budding) whereas sexual reproductive effort can be considerably higher (Hunter 1984). Asexual reproduction can be an advantageous strategy under conditions of frequent environmental disturbance and or high mortality of small sized colonies (Nakamaru et al. 2007). The small reproductive effort required for asexual budding in anemones, along with environmental disturbances could help explain the shifts from scleractinian species to more soft-bodied cnidarian species noted by Norstrom et al. (2009) and Dudgeon et al. (2010).

The additional energy needed to support increased budding rates for anemones hosting strains 1 and 2 (Fig. 3d) may be explained by the higher translocation rates of these symbionts with increased carbon availability. Interestingly, for the strain 3 holobiont, the rate of photosynthate received by the host did not vary, suggesting that the energetic requirement for the increase in budding rates observed at high $p\text{CO}_2$ may have had a different origin. Host carbonic anhydrases, a central component of the carbon concentrating mechanism (CCM), are important for supplying inorganic carbon to the symbiont for photosynthesis (Weis et al. 1989; Weis and Reynolds 1999). A change in available DIC may reduce the need for actively maintaining energetically costly CCMs within the host and symbiont (Weis et al. 1989; Weis and Reynolds 1999; Leggat et al. 2002) and could represent significant energetic savings with elevated $p\text{CO}_2$, particularly to the host. Such down-regulation of animal derived CCM's may have occurred in the strain 3 holobiont combination used here, with the energetic surplus being reallocated toward greater budding rates as well. Similarly, reallocation of energetic savings may have played a role in the other two host: symbiont combinations. The benefits of energy reallocation have been reported for the alga *Chlorella pyrenoidosa* and *Chlamydomonas reinhardtii*, where reductions in CA activity due to elevated $p\text{CO}_2$ occurred in concert with increases in protein and carbohydrate concentrations, thus boosting energetic reserves within the cell (Xia and Gao 2005). Reductions in host CAs have been observed for some scleractinian coral species under high CO_2 conditions as well (Moya and Miller 2012). In this regard, further studies that incorporate total carbon budgets (*sensu* Tremblay et al. 2013), respiratory demand, and quantify specific biomass from protein, lipids and carbohydrates could contribute substantially to future investigations of how elevated $p\text{CO}_2$ will impact different *Symbiodinium*-based symbioses.

Interestingly, despite the close genetic relationship among the three symbiont strains and two host populations, unique differences were nevertheless observed among the three host/symbiont combinations. Differences in cell density, within the ambient treatments, were segregated between the

two host anemone populations as the strain 3-host: symbiont combination (collected from Bermuda) was significantly higher than strains 1 and 2 (in the CC7 clone). As discussed previously, this likely influenced differences in translocation to the host, and may suggest the host as a major driving factor with respect to changes in physiology in response to elevated $p\text{CO}_2$. However, differences in symbiont physiology were also observed both with respect to chlorophyll content and photosynthetic yields, indicating that significant physiological differences can exist even among clonal variants and that these differences may also influence the holobiont response to climate change. How anemones, along with other sessile marine invertebrates, respond to elevated CO_2 and the potential ecological implications of greater asexual budding rates within these clonal organisms will become increasingly important toward understanding future coral reefs under high atmospheric CO_2 conditions. Likewise, whether host vs. symbiont physiological changes can be ranked differently in terms of importance to the overall holobiont response to climate change will become an increasingly important area of *Symbiodinium* symbiosis biology.

References

- Alexandre, A., J. Silva, P. Buapet, M. Björk, and R. Santos. 2012. Effects of CO_2 enrichment on photosynthesis, growth, and nitrogen metabolism of the seagrass *Zostera noltii*. *Ecol. Evol.* 2: 2625–2635. doi:10.1002/ece3.333
- Beardall, J., S. Stojkovic, and S. Larsena. 2009. Living in a high CO_2 world: Impacts of global climate change on marine phytoplankton. *Plant Ecol. Divers.* 2: 191–205. doi:10.1080/17550870903271363
- Brading, P., M. E. Warner, P. Davey, D. J. Smith, E. P. Achterberg, and D. J. Suggett. 2011. Differential effects of ocean acidification on growth and photosynthesis among phylogenetic types of *Symbiodinium* (Dinophyceae). *Limnol. Oceanogr.* 56: 927–938. doi:10.4319/lo.2011.56.3.0927
- Clayton, W. S. 1985. Pedal laceration by the anemone *Aiptasia pallida*. *Mar. Ecol. Prog. Ser.* 21: 75–80. doi:10.3354/meps021075
- Clayton, W. S., and H. R. Lasker. 1985. Individual and population growth in the asexually reproducing anemone *Aiptasia pallida* Verrill. *J. Exp. Mar. Biol. Ecol.* 90: 249–58. doi:10.1016/0022-0981(85)90170-4
- Coffroth, M. A., and S. R. Santos. 2005. Genetic diversity of symbiotic dinoflagellates in the genus *Symbiodinium*. *Protist* 156: 19–34. doi:10.1016/j.protis.2005.02.004
- Cohen, A. L., and M. Holcomb. 2009. Why corals care about ocean acidification: Uncovering the mechanism. *Oceanography* 22: 118–127. doi:10.5670/oceanog.2009.102
- Comeau, S., P. J. Edmunds, N. B. Spindel, and R. C. Carpenter. 2013. The responses of eight coral reef calcifiers to increasing partial pressure of CO_2 do not exhibit a tipping point. *Limnol. Oceanogr.* 58: 388–398. doi:10.4319/lo.2013.58.1.0388
- Crawley, A., D. Kline, S. Dunn, K. Anthony, and S. Dove. 2010. The effect of ocean acidification on symbiont photorespiration and productivity in *Acropora formosa*. *Glob. Chang. Biol.* 16: 851–863. doi:10.1111/j.1365-2486.2009.01943.x
- Davy, S. K., and C. Cook. 2001. The relationship between nutritional status and carbon flux in the zooxanthellate sea anemone, *Aiptasia pallida*. *Mar. Biol.* 139: 999–1005.
- Dubinsky, Z., and I. Berman-Frank. 2001. Uncoupling primary production from population growth in photosynthesizing organisms in aquatic ecosystems. *Aquat. Sci.* 63: 4–17. doi:10.1007/PL00001343
- Dudgeon, S. R., R. B. Aronson, J. F. Bruno, and W. F. Precht. 2010. Phase shifts and stable states on coral reefs. *Mar. Ecol. Prog. Ser.* 413: 201–216. doi:10.3354/meps08751
- Edmunds, P. J., R. C. Carpenter, and S. Comeau. 2013. Understanding the threats of ocean acidification to coral reefs. *Oceanography* 26: 149–152. doi:10.5670/oceanog.2013.57
- Fabricius, K. E., and others. 2011. Losers and winners in coral reefs acclimatized to elevated carbon dioxide concentrations. *Nat. Clim. Chang.* 1: 165–169. doi:10.1038/NCLIMATE1122
- Finney, J. C., D. T. Pettay, E. M. Sampayo, M. E. Warner, H. A. Oxenford, and T. C. LaJeunesse. 2010. The relative significance of host-habitat, depth, and geography on the ecology, endemism, and speciation of coral endosymbionts in the genus *Symbiodinium*. *Microb. Ecol.* 60: 250–263. doi:10.1007/s00248-010-9681-y
- Fu, F.-X., M. E. Warner, Y. Zhang, Y. Feng, and D. A. Hutchins. 2007. Effects of increased temperature and CO_2 on photosynthesis, growth, and elemental ratios in marine *Synechococcus* and *Prochlorococcus* (Cyanobacteria). *J. Phycol.* 43: 485–496. doi:10.1111/j.1529-8817.2007.00355.x
- Gibbin, E. M., and S. K. Davy. 2014. The photo-physiological response of a model cnidarian-dinoflagellate symbiosis to CO_2 -induced acidification at the cellular level. *J. Exp. Mar. Biol. Ecol.* 457: 1–7. doi:10.1016/j.jembe.2014.03.015
- Goulet, T. L., C. B. Cook, and D. Goulet. 2005. Effect of short-term exposure to elevated temperatures and light levels on photosynthesis of different host-symbiont combinations in the *Aiptasia pallida/Symbiodinium* symbiosis. *Limnol. Oceanogr.* 50: 1490–1498. doi:10.4319/lo.2005.50.5.1490
- Grajales, A. G., and E. Rodriguez. 2014. Morphological revision of the genus *Aiptasia* and the family Aiptasiidae (Cnidaria, Actinaria, Metridioidea). *Zootaxa.* 3826: 55–100. doi:10.11646/zootaxa.3826.1.2
- Grottoli, A. G., and others. 2014. The cumulative impact of annual coral bleaching can turn some coral species winners into losers. *Glob. Chang. Biol.* 20: 3823–3833. doi:10.1111/gcb.12658
- Guinotte, J. M., and V. J. Fabry. 2008. Ocean acidification and its potential effects on marine ecosystems. *Ann. N. Y. Acad. Sci.* 1134: 320–342. doi:10.1196/annals.1439.013

- Hennige, S. J., M. P. McGinley, A. G. Grottoli, and M. E. Warner. 2011. Photoinhibition of *Symbiodinium* spp. within the reef corals *Montastraea faveolata* and *Porites astreoides*: Implications for coral bleaching. *Mar. Biol.* 158: 2515–2526. doi:10.1007/s00227-011-1752-1
- Hofmann, G. E., J. P. Barry, P. J. Edmunds, R. D. Gates, D. A. Hutchins, T. Klinger, and M. A. Sewell. 2010. The effect of ocean acidification on calcifying organisms in marine ecosystems: An organism-to-ecosystem perspective. *Annu. Rev. Ecol. Evol. Syst.* 41: 127–147. doi:10.1146/annurev.ecolsys.110308.120227
- Huang, X. Q., and A. Madan. 1999. CAP3: A DNA sequence assembly program. *Genome Res.* 9: 868–877. doi:10.1101/gr.9.9.868
- Hunter, T. 1984. The energetics of asexual reproduction: Pedal laceration in the symbiotic sea anemone *Aiptasia pulchella* (Carlgren, 1943). *J. Exp. Mar. Biol. Ecol.* 83: 127–147. doi:10.1016/0022-0981(84)90041-8
- Hurd, C. L., C. D. Hepburn, K. I. Currie, J. A. Raven, and K. A. Hunter. 2009. Testing the effects of ocean acidification on algal metabolism: Considerations for experimental design. *J. Phycol.* 45: 1236–1251. doi:10.1111/j.1529-8817.2009.00768.x
- Hutchins, D. A., and others. 2007. CO₂ control of *Trichodesmium* N₂ fixation, photosynthesis, growth rates, and elemental ratios: Implications for past, present, and future ocean biogeochemistry. *Limnol. Oceanogr.* 52: 1293–1304. doi:10.4319/lo.2007.52.4.1293
- Iglesias-Prieto, R., and R. K. Trench. 1997. Acclimation and adaptation to irradiance in symbiotic dinoflagellates. II. Response of chlorophyll-protein complexes to different photon-flux densities. *Mar. Biol.* 130: 23–33. doi:10.1007/s002270050221
- Iglesias-Rodriguez, M. D., and others. 2008. Phytoplankton calcification in a high-CO₂ world. *Science* 320: 336–340. doi:10.1126/science.1154122
- IPCC. 2013. Summary for policymakers. In T. F. Stocker, D. Qin, G.-K. Plattner, M. Tignor, S. K. Allen, J. Boschung, A. Nauels, Y. Xia, V. Bex and P. M. Midgley [eds.], *Climate Change 2013: The Physical Science Basis. Contribution of Working Group I to the Fifth Assessment Report of the Intergovernmental Panel on Climate Change*. Cambridge Univ. Press.
- Kaniewska, P., P. R. Campbell, D. I. Kline, M. Rodriguez-Lanetty, D. J. Miller, S. Dove, and O. Hoegh-Guldberg. 2012. Major cellular and physiological impacts of ocean acidification on a reef building coral. *PLoS one.* 7: 1–12. doi:10.1371/journal.pone.0034659
- Koch, M., G. Bowes, C. Ross, and X. Zhang. 2013. Climate change and ocean acidification effects on seagrasses and marine macroalgae. *Glob. Chang. Biol.* 19: 103–132. doi:10.1111/j.1365-2486.2012.02791.x
- LaJeunesse, T. C. 2001. Investigating the biodiversity, ecology, and phylogeny of endosymbiotic dinoflagellates in the genus *Symbiodinium* using the its region: In search of a “species” level marker. *J. Phycol.* 37: 866–880. doi:10.1046/j.1529-8817.2001.01031.x
- LaJeunesse, T. C. 2012. Diversity and community structure of symbiotic dinoflagellates from Caribbean coral reefs. *Mar. Biol.* 141: 387–400. doi:10.1007/s00227-002-0829-2
- LaJeunesse, T. C., J. E. Parkinson, and J. D. Reimer. 2012. A genetics-based description of *Symbiodinium minutum* sp. nov. and *S. psygmophilum* sp. nov. (Dinophyceae), two dinoflagellates symbiotic with cnidaria. *J. Phycol.* 48: 1380–1391. doi:10.1111/jpy.12168
- Langdon, C., and M. J. Atkinson. 2005. Effect of elevated pCO₂ on photosynthesis and calcification of corals and interactions with seasonal change in temperature/irradiance and nutrient enrichment. *J. Geophys. Res.* 110: 1–16. doi:10.1029/2004JC002576
- Leal, M. C., K. Hoadley, D. T. Pettay, A. Grajales, R. Calado, and M. E. Warner. 2015. Symbiont type influences trophic plasticity of a model cnidarian-dinoflagellate symbiosis. *J. Exp. Biol.* 218: 858–863. doi:10.1242/jeb.115519
- Leggat, W., M. R. Badger, and D. Yellowlees. 1999. Evidence for an inorganic carbon-concentrating mechanism in the symbiotic dinoflagellate *Symbiodinium* sp. *Plant Physiol.* 121: 1247–1255. doi:10.1104/pp.121.4.1247
- Leggat, W., E. M. Marendy, B. Baillie, S. M. Whitney, M. Ludwig, M. R. Badger, and D. Yellowlees. 2002. Dinoflagellate symbioses: Strategies and adaptations for the acquisition and fixation of inorganic carbon. *Funct. Plant Biol.* 29: 309–322. doi:10.1071/PP01202
- Lehnert, E. M., M. S. Burriesci, and J. R. Pringle. 2012. Developing the anemone *Aiptasia* as a tractable model for cnidarian-dinoflagellate symbiosis: The transcriptome of aposymbiotic *A. pallida*. *BMC Genomics* 13: 271. doi:10.1186/1471-2164-13-271
- Lewis, E., D. Wallace, and L. J. Allison. 1998. *Program developed for CO₂ system calculations*. Carbon Dioxide Information Analysis Center, managed by Lockheed Martin Energy Research Corporation for the US Department of Energy. Available from <http://cdiac.esd.ornl.gov/oceans/co2rprtnbk>. Accessed on August 31 2014.
- Li, G., and D. A. Campbell. 2013. Rising CO₂ interacts with growth light and growth rate to alter photosystem II photoinactivation of the coastal diatom *Thalassiosira pseudonana*. *PLoS ONE* 8. doi:10.1371/journal.pone.0055562
- Luthi, D., and others. 2008. High-resolution carbon dioxide concentration record 650,000–800,000 years before present. *Nature* 453: 379–382. doi:10.1038/nature06949
- Martins, W. S., Lucas, D. C. S., de Souza Neves, K. F., and D. J. Bertioli. 2009. WebStat A web software for microsatellite marker development. *Bioinformatics.* 3: 282–283. ISSN 0973-2063
- Marubini, F., and P. S. Davies. 1996. Nitrate increases zooxanthellae population density and reduces skeletogenesis in corals. *Mar. Biol.* 127: 319–28. doi:10.1007/BF00942117

- Moya, A., and D. J. Miller. 2012. Whole transcriptome analysis of the coral *Acropora millepora* reveals complex responses to CO₂-driven acidification during the initiation of calcification. *Mol. Ecol.* 21: 2440–2454. doi:10.1111/j.1365-294X.2012.05554.x
- Muller-Parker, G. 1984. Photosynthesis-irradiance responses and photosynthetic periodicity in the sea-anemone *Aiptasia-pulchella* and its zooxanthellae. *Mar. Biol.* 82: 225–232. doi:10.1007/BF00392403
- Nakamaru, M., Y. Beppu, and K. Tsuji. 2007. Does disturbance favor dispersal? An analysis of ant migration using the colony-based lattice model. *J. Theor. Biol.* 248: 288–300. doi:10.1016/j.jtbi.2007.05.012
- Norstrom, A. V., M. Nystrom, J. Lokrantz, and C. Folke. 2009. Alternative states on coral reefs: Beyond coral-macroalgal phase shifts. *Mar. Ecol. Prog. Ser.* 376: 295–306. doi:10.3354/meps07815
- Pettay, D. T., and T. C. LaJeunesse. 2007. Microsatellites from clade B *Symbiodinium* spp. specialized for Caribbean corals in the genus *Madracis*. *Mol. Ecol. Notes* 7: 1271–1274. doi:10.1111/j.1471-8286.2007.01852.x
- Pettay, D. T., and T. C. LaJeunesse. 2009. Microsatellite loci for assessing genetic diversity, dispersal and clonality of coral symbionts in ‘stress-tolerant’ clade D *Symbiodinium*. *Mol. Ecol. Resour.* 9: 1022–1025. doi:10.1111/j.1755-0998.2009.02561.x
- Pettay, D. T., and T. C. LaJeunesse. 2013. Long-range dispersal and high-latitude environments influence the population structure of a “stress-tolerant” dinoflagellate endosymbiont. *PLoS ONE* 8. doi:10.1371/journal.pone.0079208
- Porra, R. J., W. A. Thompson, and P. E. Kriedemann. 1989. Determination of accurate extinction coefficients and simultaneous equations for assaying chlorophylls *a* and *b* extracted with four different solvents: Verification of the concentration of chlorophyll standards by atomic absorption spectroscopy. *Biochim. Biophys. Acta* 975: 384–394. doi:10.1016/S0005-2728(89)80347-0
- Rozen, S. and H. Skaletsky. 2000. Primer3 on the WWW for general users and for biologist programmers. *Methods Mol. Biol.* 132: 365–386. doi:10.1385/1-59259-192-2:365
- Sampayo, E. M., T. Ridgeway, P. Bongaerts, and O. Hoegh-Gulberg. 2008. Bleaching susceptibility and mortality of corals are determined by fine-scale differences in symbiont type. *Proc. Natl. Acad. Sci. USA* 105: 10444–10449. doi:10.1073/pnas.0708049105
- Sampayo, E. M., S. Dove, and T. C. LaJeunesse. 2009. Cohesive molecular genetic data delineate species diversity in the dinoflagellate genus *Symbiodinium*. *Mol. Ecol.* 18: 500–519. doi:10.1111/j.1365-294X.2008.04037.x
- Santos, S. R. and M. A. Coffroth. 2003. Molecular genetic evidence that dinoflagellates belonging to the genus *Symbiodinium* Freudenthal are haploid. *Biol. Bull.* 204: 10–20. doi:10.2307/1543491
- Santos, S. R., C. Gutierrez-Rodriguez, and M. A. Coffroth. 2003. Phylogenetic identification of symbiotic dinoflagellates via length heteroplasmy in domain V of chloroplast large subunit (cp23S)-ribosomal DNA sequences. *Mar. Biotechnol.* 5: 130–140. doi:10.1007/s10126-002-0076-9
- Schoenberg, D., and R. Trench. 1980. Genetic variation in *Symbiodinium* (*Symbiodinium*) *microadriaticum* Freudenthal, and specificity in its symbioses with marine invertebrates. I. Isoenzyme and soluble protein patterns of axenic cultures of *Symbiodinium microadriaticum*. *Proc. R. Soc. A* 207: 405–427. doi:10.1098/rspb.1980.0031
- Schoepf, V., and others. 2013. Coral energy reserves and calcification in a high-CO₂ world at two temperatures. *PLoS ONE* 8: e75049. doi:10.1371/journal.pone.0075049
- Smith, P. K., and others. 1985. Determination of protein concentration by the bicinchoninic acid method. *Anal. Biochem.* 150: 76–85. doi:10.1016/0003-2697(85)90442-7
- Suggett, D. J., L. F. Dong, T. Lawson, E. Lawrenz, L. Torres, and D. J. Smith. 2012a. Light availability determines susceptibility of reef building corals to ocean acidification. *Coral Reefs* 32: 327–337. doi:10.1007/s00338-012-0996-7
- Suggett, D. J., and others. 2012b. Sea anemones may thrive in a high CO₂ world. *Glob. Chang. Biol.* 18: 3015–3025. doi:10.1111/j.1365-2486.2012.02767.x
- Sunagawa, S., and others. 2009. Generation and analysis of transcriptomic resources for a model system on the rise: The sea anemone *Aiptasia pallida* and its dinoflagellate endosymbiont. *BMC Genomics* 10: 258. doi:10.1186/1471-2164-10-258
- Thornhill, D. J., Y. Xiang, D. T. Pettay, M. Zhong, and S. R. Santos. 2013. Population genetic data of a model symbiotic cnidarian system reveal remarkable symbiotic specificity and vectored introductions across ocean basins. *Mol. Ecol.* 22: 4499–4515. doi:10.1111/mec.12416
- Towanda, T., and E. V. Thuesen. 2012. Prolonged exposure to elevated CO₂ promotes growth of the algal symbiont *Symbiodinium muscatinei* in the intertidal sea anemone *Anthopleura elegantissima*. *Open Biol.* 1: 615–621. doi:10.1242/bio.2012521
- Tremblay, P., M. Fine, J. F. Maguer, and R. Grover. 2013. Ocean acidification increases photosynthate translocation in a coral–dinoflagellates symbiosis. *Biogeosciences* 10: 83–109. doi:10.5194/bgd-10-83-2013
- Trench, R. 1993. Microalgal-invertebrate symbioses: A review. *Endocytobiosis Cell Resour.* 9: 135–175.
- Voolstra, C. R. 2013. A journey into the wild of the cnidarian model system *Aiptasia* and its symbionts. *Mol. Ecol.* 22: 4366–4368. doi:10.1111/mec.12464
- Wall, C. B., T. Y. Fan, and P. J. Edmunds. 2014. Ocean acidification has no effect on thermal bleaching in the coral *Seriatopora caliendrum*. *Coral Reefs* 33: 119–130. doi:10.1007/s00338-013-1085-2
- Warner, M. E., and S. Berry-Lowe. 2006. Differential xanthophyll cycling and photochemical activity in symbiotic

- dinoflagellates in multiple locations of three species of Caribbean coral. *J. Exp. Mar. Biol. Ecol.* 339: 86–95. doi: [10.1016/j.jembe.2006.07.011](https://doi.org/10.1016/j.jembe.2006.07.011)
- Weis, V. M. 1993. Effect of dissolved inorganic carbon concentration on the photosynthesis of the symbiotic sea anemone *Aiptasia pulchella* Carlgren: Role of carbonic anhydrase. *J. Exp. Mar. Biol. Ecol.* 174: 209–225. doi: [10.1016/0022-0981\(93\)90018-J](https://doi.org/10.1016/0022-0981(93)90018-J)
- Weis, V. M., G. J. Smith, and L. Muscatine. 1989. A CO₂ supply mechanism in zooxanthellate cnidarians—role of carbonic-anhydrase. *Mar. Biol.* 100: 195–202. doi: [10.1007/BF00391958](https://doi.org/10.1007/BF00391958)
- Weis, V. M., and W. S. Reynolds. 1999. Carbonic anhydrase expression and synthesis in the sea anemone *Anthopleura elegantissima* are enhanced by the presence of dinoflagellate symbionts. *Physiol. Biochem. Zool.* 72: 307–316. doi: [10.1086/316674](https://doi.org/10.1086/316674)
- Wham, D. C., D. T. Pettay, and T. C. LaJeunesse. 2011. Microsatellite loci for the host-generalist “zooxanthella” *Symbiodinium trenchi* and other Clade D *Symbiodinium*. *Conserv. Genet. Resour.* 3: 541–544. doi: [10.1007/s12686-011-9399-2](https://doi.org/10.1007/s12686-011-9399-2)
- Wooldridge, S. A. 2009. A new conceptual model for the warm-water breakdown of the coral-algae endosymbiosis. *Mar. Freshwater Res.* 60: 483–496. doi: [10.1071/MF08251](https://doi.org/10.1071/MF08251)
- Xia, J. R., and K. S. Gao. 2005. Impacts of elevated CO₂ concentration on biochemical composition, carbonic anhydrase, and nitrate reductase activity of freshwater green algae. *J. Integr. Plant Biol.* 47: 668–675. doi: [10.1111/j.1744-7909.2005.00114.x](https://doi.org/10.1111/j.1744-7909.2005.00114.x)
- Yao, W., and R. H. Byrne. 1998. Simplified seawater alkalinity analysis: Use of linear array spectrometers. *Deep-Sea Res. PT I.* 45: 1383–1392. doi: [10.1016/S0967-0637\(98\)00018-1](https://doi.org/10.1016/S0967-0637(98)00018-1)
- Zimmerman, R. C., D. G. Kohrs, D. L. Steller, and R. S. Alberte. 1997. Impacts of CO₂ enrichment on productivity and light requirements of Eelgrass. *Plant Physiol.* 115: 599–607. doi: [10.1104/pp.115.2.599](https://doi.org/10.1104/pp.115.2.599)

Acknowledgments

We thank Dr. John Pringle for the generous donation of the CC7 aposymbiotic anemones and Dr. Mary Alice Coffroth and the Buffalo Undersea Reef Research (BURR) culture collection for the *Symbiodinium minutum* cultures. This work was supported by the National Science Foundation (awards 104940 and 1316055) to M.E.W.

Submitted 10 November 2014

Revised 25 May 2015, 25 July 2015

Accepted 3 August 2015

Associate editor: James Leichter